Vol 14 No 3, March 2005
1009-1963/2005/14(03)/0511-05

Chinese Physics

© 2005 Chin. Phys. Soc.
and IOP Publishing Ltd

Measurement of hyperfine structure and isotope shifts in the 580.56nm line of $^{142-145,146,148,150}$Nd^{+} *

Ma Hong-Liang(马洪良)†

Department of Physics, Shanghai University, Shanghai 200436, *China*

(Received 11 February 2004; revised manuscript received 6 September 2004)

Isotope shifts and hyperfine spectrum of singly ionized neodymium ion was measured by collinear fast-ion-beam laser spectroscopy. The hyperfine A constants and B constants are obtained for the $(23230)^{o}_{9/2}$ level and $4f^{4}5d\ ^{6}K_{9/2}$ level, respectively. The optical isotope shifts between seven isotopes in the 580.56 nm of $^{142-145,146,148,150}$Nd^{+} line are determined. The configuration admixtures for $(23230)^{o}_{9/2}$ level were quantitatively analysed to be $4f^{4}6p$, $4f^{3}5d^{2}$, and $4f^{3}5d6p$ with mixing coefficients of 67%, 5%, and 28%, respectively.

Keywords: isotope shifts, hyperfine structure, fast-ion-beam laser spectroscopy, hyperfine coupling constants

PACC: 3290

1. Introduction

In recent years, many works were contributed to the measurement of hyperfine structure (HFS) and isotope shifts.[1−3] Hyperfine structure in atomic ions is caused by the electromagnetic interaction between the nucleus and orbital electrons. Not only the information of nuclear structure but also electronic properties of ions can be obtained through studying the HFS of ions. Thus, hyperfine structure of singly charged ions has been extensively investigated for many ions and much information has been obtained.[4,5] The collinear geometry technique provides a powerful method of high precision spectroscopy. Because of the kinematic compression when ions are accelerated, sub-Doppler resolution can be obtained with a collinear geometry. The use of isotope separator permits selective measurement of different isotopes. These two properties make the collinear fast-ion-beam laser spectroscopy very powerful and accurate. Collinear ion-beam laser spectroscopy has been used for hyperfine structure measurement of La II[6] and Tb II.[7]

Hyperfine energy level splitting is a result of the interaction between valence electron and the nucleus. In first order perturbation theory, the hyperfine energy splitting ΔE is expressed as the sum of magnetic dipole term $\Delta E_{\rm MD}$ and the electric quadruple term $\Delta E_{\rm EQ}$ as follows:[8]

$$\begin{aligned}\Delta E =&\Delta E_{\rm MD} + \Delta E_{\rm EQ},\\ =&\frac{1}{2}KA + \frac{\frac{3}{4}K(K+1) - I(I+1)J(J+1)}{2I(2I-1)J(2J-1)}B, \quad (1)\end{aligned}$$

where

$$K = F(F+1) - I(I+1) - J(J+1). \quad (2)$$

The F is the total angular momentum, $F = I + J$; I and J are the nuclear spin and the total electronic angular quantum numbers, respectively. A and B are the magnetic dipole and electric quadruple coupling constants, respectively. The energy shift $\Delta E_{\rm MD}$ is caused by the interaction between the internal magnetic field produced at the nucleus by orbital electrons and the nuclear magnetic dipole moment. $\Delta E_{\rm EQ}$ corresponds to the interaction between the electric field gradient and the nuclear quadruple moment.

Accurate rare-earth abundances are of interest in the study of chemically peculiar stars. Therefore an accurate knowledge of hyperfine structure of rare-earth is necessary.[9] Nd has five stable even isotopes

*Project supported by the National Natural Science Foundation of China (Grant No 19274049) and Shanghai Leading Academic Discipline Program.

†E-mail: hl-ma@mail.shu.edu.cn

and two odd isotopes, and both odd isotopes ^{143}Nd and ^{145}Nd have nuclear spin $I = \frac{7}{2}$. There are about one thousand of even and odd energy levels of singly ionized neodymium known.[10,11] The isotope shifts between $^{144}Nd^+$ and $^{150}Nd^+$ in the energy range from 2700 to 27000cm^{-1} were measured by Fourier transform spectroscopy[10] and those between $^{142}Nd^+$ and $^{144}Nd^+$ at the spectral lines of 393–476nm were measured by the traditional interferometric technique,[11] with uncertainty of tens to hundreds of MHz. In this work, the hyperfine A and B constants for $^{143}Nd^+$ and $^{145}Nd^+$ and isotope shifts between even stable isotopes $^{142-146,148,150}Nd^+$ in 580.56nm spectral line were determined using collinear fast-ion-beam laser spectroscopy.

2. Experimental methods and results

The experimental setup is shown in Fig.1. A 30kV electronic isotope separator (Danfysik 1080-30) was used to produce a singly ionized neodymium ion beam. The ions were produced in a low-voltage electron-impact hollow cathode ion source (Danfysik 911A) operated at a gas pressure of about 2×10^{-3}Pa, focused by an electrostatic lens and injected into an analysing magnet, and an isotopically pure ion beam was selected. The ion current was monitored by a Faraday cup after the interaction region. The beam current was typically of the order of 1–2μA when neodymium chloride was used as a precursor in the ion source. In order to avoid collision quenching, collision-induced ion beam excitation and radiation trapping, the chamber vacuum was kept below 3×10^{-5}Pa.

A single-mode Coherent 899-29 Autoscan ring dye laser was used to provide light with a bandwidth less than 1MHz. The dye laser was pumped by an Innova Sabre Ar-ion laser at a wavelength of 514.5nm. The laser beam was steered through a Browster window into the chamber and then through a set of apertures that define the ion beam path to obtain a good antiparallel overlap between the laser and Nd^+ ion beams in the detection region. The dye used in this work was Rhodamine 6G. The frequency of the dye laser was measured by a home-made wavemeter calibrated by the iodine absorption spectrum. A 100-cm confocal Fabry–Perot interferometer (FPI) with free spectral range 146.5±0.1MHz was used to accurately calibrate the fluorescence spectra and check for scan nonlinearities. To prevent the depletion of the metastable state by laser light before the ion beam enters the chamber, a three-part post-acceleration electrode structure was placed in the chamber. The two outer discs were electrically grounded and the middle one was held at a negative potential of 1000V, where the ions are accelerated locally. Because of the different Doppler shifts, the ions outside of the electrode structure are not affected by the laser, and they are typically off resonance by ~7.5GHz. Keeping the post-acceleration potential fixed, the laser is scanned to bring it into resonance with the ions. Stray light from the laser beam was suppressed by an appropriate combination of a broad-band filter and a monochromator. The fluorescence light was focused by a set of lens and detected by a photomultiplier (EMI 9789B). The fluorescence from the laser-excited ion beam and signals from two photodiodes accepting the transmitted light through the FPI and the iodine cell were simultaneously recorded by the three-input multichannel analyser.

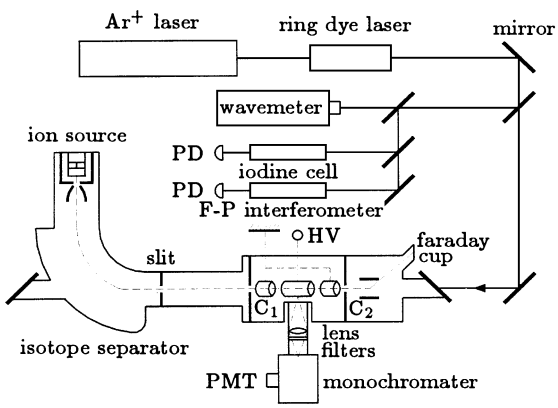


Fig.1. Schematic of collinear Nd ion-beam-laser apparatus. PMT, PD, and HV are the abbreviations for photomultiplier tube, photodiode, and high-voltage, respectively.

The energy-level diagram in Nd II investigated is shown in Fig.2, where the laser-excited optical transitions from the metastable levels are indicate by upward arrows. The resonant spectrum for $^{142-146,148,150}$Nd II from the metastable $4f^45d\ ^6K_{9/2}$ level to the excited level $(23230)^{\circ}_{9/2}$ is shown in Fig.3. Typical hyperfine spectrum of $^{143}Nd^+$ is shown in Fig.4. All the hyperfine components are resolved and assigned. The isotope shifts between seven stable isotopes of Nd II in the 580.56nm spectral line are presented in Table 1. The quoted error 9MHz comes from the uncertainties of determining the centres of iodine absorption peaks and the reso-

nant peaks. The magnetic-dipole constant A and the electric-quadrupole constant B were derived from the measured hyperfine spectra. The results are shown in Table 2.

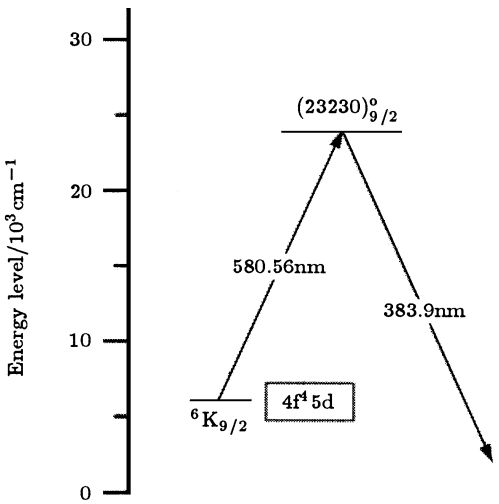


Fig.2. Energy levels of Nd II investigated in this work. The laser induced transition from the metastable $4f^45d$ configuration is indicated by the upward arrow.

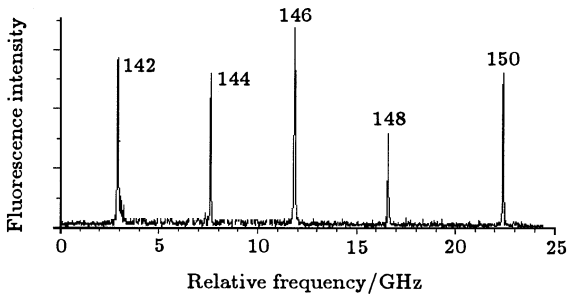


Fig.3. Measured fluorescence spectrum in the line 580.56nm of Nd II.

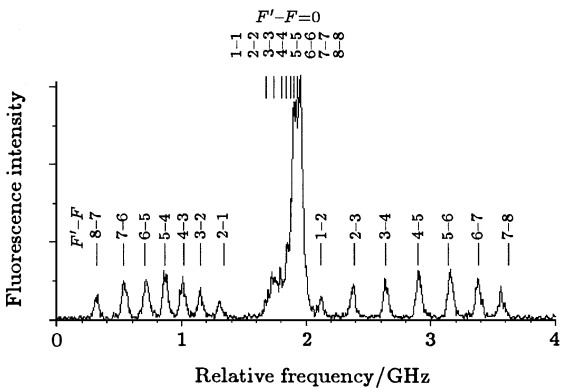


Fig.4. Hyperfine structure spectrum in the 580.56 nm line of $^{143}Nd^+$. F and F' are the total angular momentum of the upper level and lower level, respectively.

Table 1. Isotope shifts (Δ_{IS}) and modified isotope shifts (Δ_{MIS}) in 580.56nm line and Δ_{MIS} for $4f^46s$–$4f^45d$ transition in Nd II.

Isotope pairs	580.56nm		$4f^46s$–$4f^45d$[12]
	Δ_{IS}/MHz	Δ_{MIS}/MHz	Δ_{MIS}/MHz
142–144	1221(9)	1185	–1998
144–146	1110(9)	1110	–1902
146–148	1326(9)	1365	–2190
148–150	2007(9)	2118	–3051
142–143	558(9)	1074	–1881
144–145	420(9)	831	–1644

Table 2. Measured hyperfine A and B constants in the line 580.56nm of $^{143,145}Nd^+$.

λ/nm	J	level/cm^{-1}	A/MHz		B/MHz	
			$^{143}Nd^+$	$^{145}Nd^+$	$^{143}Nd^+$	$^{145}Nd^+$
580.56	9/2	6005	–200.2 ± 1.5	–124.1 ± 1.4	–120.5 ± 8.1	65.7 ± 11.8
	9/2	23230	–197.2 ± 0.7	–121.1 ± 1.2	–106.1 ± 9.4	–52.0 ± 9.1

3. Determination of configuration of admixture

The isotope shift (Δ_{IS}) is assumed to be the sum of the field shift (Δ_{FS}) depending on the nuclear charge distribution, and the mass shift (Δ_{MS}) caused by the difference in nuclear mass. Δ_{MS} is defined to be the sum of the normal mass shift (Δ_{NMS}) and specific mass shift (Δ_{SMS}). A King plot is constructed to separate the Δ_{NMS}, Δ_{SMS} and Δ_{FS} from the measured Δ_{IS}. Isotopes 144 and 146 of Nd II are taken as a standard pair. The modified isotope shift between

an isotope pair with mass numbers γ and $\gamma'(\gamma' > \gamma)$ is

$$\Delta\nu(MIS)_{\gamma\gamma'} = \mu_{\gamma\gamma'} \times \Delta\nu(IS)_{\gamma\gamma'}, \qquad (3)$$

where the modifying factor $\mu_{\gamma\gamma'}$ is defined as $\mu_{\gamma\gamma'} = \dfrac{2 \times \gamma \times \gamma'}{144 \times 146 \times (\gamma' - \gamma)}$. The modified isotope shift in spectral line 580.56nm is listed in Table 1, together with the modified isotope shift for $4f^4 6s$–$4f^4 5d$ transition in Nd II.[12] The King plot of the modified isotope shift in spectral line 580.56 nm against that for $4f^4 6s$–$4f^4 5d$ transition was shown in Fig.5, where the solid line is a least-square fit. In order to derive absolute values of $\Delta_{\rm FS}$, it has to be known for one transition and then the field shifts for other transitions can be determined by means of the King parameters obtained from the slopes of the fitted lines. The field shift for the standard pair for $4f^4 6s$–$4f^4 5d$ transition in Nd II is known as –2031MHz.[12] For the standard pair $^{144}Nd^+$ and $^{146}Nd^+$, the field shift in the line 580.56nm is 1806MHz, the normal mass shift, the specific mass shift, and field shift between two isotopes in the line 580.56 nm were separated from the measured isotope shift and listed in Table 3.

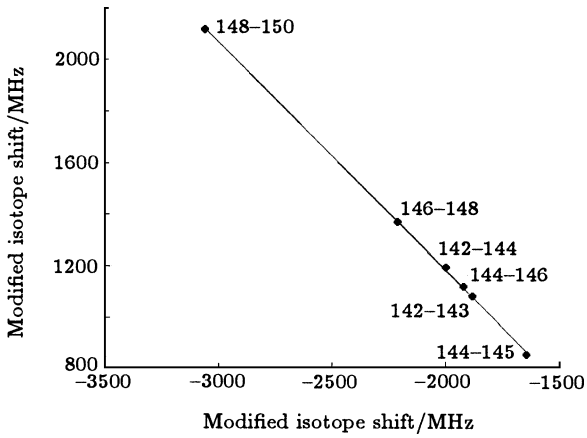


Fig.5. The King plot. The modified isotope shifts in the line 580.56nm (this work) are plotted against those for $4f^4 6s$–$4f^4 5d$ transition. The solid line is a least-square fit.

Table 3. $\Delta_{\rm IS}$, $\Delta_{\rm MS}$, $\Delta_{\rm NMS}$, $\Delta_{\rm SMS}$ and $\Delta_{\rm FS}$ in the line 580.56nm in Nd II.

Isotope pairs	$\Delta_{\rm IS}$/MHz	$\Delta_{\rm MS}$/MHz	$\Delta_{\rm NMS}$/MHz	$\Delta_{\rm SMS}$/MHz	$\Delta_{\rm FS}$/MHz
142–144	1221(9)	–744	27	–771	1965
144–146	1110(9)	–723	27	–750	1833
146–148	1326(9)	–702	27	–729	2028
148–150	2007(9)	–684	24	–708	2691
142–143	558(9)	–384	15	–390	933
144–145	420(9)	–363	12	–375	783

It is reasonable to consider that the excited level $(23230)^{\circ}_{9/2}$ consists of $4f^4 6p$, $4f^3 5d^2$ and $4f^3 5d6s$.[12] According to the "sharing rule", for a given mixing level, the contribution to the isotope shift of each pure configuration is proportional to its mixing probability. For the $4f^4 5d\ ^6K_{9/2} - (23230)^{\circ}_{9/2}$ transition, the field shift and specific mass shift are determined by the three transitions between pure configurations: $4f^4 5d$–$4f^4 6p$, $4f^4 5d$-$4f^3 5d^2$, and $4f^4 5d$–$4f^3 5d6s$. For the standard pair $^{144}Nd^+$ and $^{146}Nd^+$, the specific mass shifts for the three transitions are –120MHz, –990MHz and –1080MHz, respectively.[12] Using the electron screening ratios based on relativistic Hartree–Fock calculation, the following ratios of field shift (FS) can be obtained,

$$\begin{aligned}
&\frac{\mathrm{FS}(4f^4 6s - 4^4 5d)}{\mathrm{FS}(4f^4 6s - 4f^4 6p)} = 1.20,\\
&\frac{\mathrm{FS}(4f^4 6s - 4f^3 5d^2)}{\mathrm{FS}(4f^4 6s - 4f^4 5d)} = -0.094,\\
&\frac{\mathrm{FS}(4f^4 6s - 4f^3 5d6s)}{\mathrm{FS}(4f^4 6s - 4f^4 5d)} = -1.21. \qquad (4)
\end{aligned}$$

Solving the above equations, for the standard pair $^{144}Nd^+$ and $^{146}Nd^+$, the field shifts for the $4f^4 5d$–$4f^4 6p$, $4f^4 5d$–$4f^3 5d^2$ and $4f^4 5d$–$4f^3 5d6s$ transitions are 339MHz, 2223MHz, and 4488MHz, respectively. Based on the sharing rule, the mixing probabilities of three $4f^4 6p$, $4f^3 5d^2$ and $4f^3 5d6s$ pure configurations are 67%, 5% and 28%, respectively.

4. Conclusion

In this work, we have presented accurate measurements of isotope shifts between seven stable isotopes in Nd II and hyperfine structure in $^{143}Nd^+$ and $^{145}Nd^+$. We have obtained improved accuracy of the isotope shift measurement and the results are in agreement with earlier measurements,[10,11] as listed in Table 4. Tentative admixtures for $(23230)^{\circ}_{9/2}$ level is deduced from derived field shift and specific mass shift using the sharing rule. The result well confirms the earlier assignment,[12] listed in Table 5.

Table 4. Comparison of isotope shifts (MHz) in this work with those from Refs.[10] and [11].

λ/nm	Lower level/cm^{-1}	Upper level/cm^{-1}	This work		From references	
			142–144	144–150	142–144	144–150
580.56	6005.271	23229.991	1218	4446	1170[11]	4260[10]

Table 5. The configuration mixing of the $(23230)^{o}_{9/2}$ level in Nd II.

Lower level	Upper level/cm^{-1}	$4f^4 6p$	$4f^3 5d^2$	$4f^3 5d6s$
$^6K_{9/2}$	23230	0.67	0.05	0.28
		0.6–0.7[12]	0.2–0[12]	0.2–0.3 [12]

References

[1] Kroger S, Basar G and Baier A 2002 *Phys. Scripta* **65** 56

[2] Rehse S J, Fairbank W M and Lee S A 2001 *J. Opt. Soc. Am.* B **18** 855

[3] Kolachevskii N N, Papchenko A A and Kiselev N A 2001 *Opt. Spectrosc.* **90** 164

[4] Villemoes P, Wang M, Arnesen A, Weiler C and Wannstrom A 1995 *Phys. Rev.* A **51** 2838

[5] Ma H L 2002 *Chin. Phys.* **11** 905

[6] Hohle C, Huhnermann H and Wagner H 1982 *Z. Phys.* A **304** 279

[7] Lawler J E, Wyart J F and Blaise J 2001 *Astrophys. J. Suppl. S.* **137** 351

[8] Emery G T 1996 "*Hyperfine Structure*" in Atomic, Molecular, and Optical Physics Handbook, G. W. F. Drake, ed. (College Park, MD: American Institute of Physics) p198

[9] Den Hartog E A, Fedchak J A and Lawler J E 2001 *J. Opt. Soc. Am.* B **18** 861

[10] Blaise J and Wyart J F 1984 *Phys. Scripta* **29** 119

[11] Ahmad S A and Saksena G D 1981 *Spectrochim. Acta* B **36** 943

[12] King W H, Steudel A and Wilson M 1973 *Z. Phys.* **265** 207